A DSB-SC SIGNAL MODEL FOR NONLINEAR REGRESSION-BASED QUADRATURE RECEIVER CALIBRATION

Roger A. Green

Elec. Eng. Dept., North Dakota State University,
P.O. Box 5285, Fargo, ND 58105-5285
Phone: (701) 231-1024, e-mail: *green@prairie.nodak.edu*

ABSTRACT

Recent advances have been made regarding quadrature receiver I/Q mismatch calibration. In particular, Green/Anderson-Sprecher/Pierre present a nonlinear regression (NLR) -based algorithm that utilizes a pure sinusoidal test signal for sensor calibration [1]. This paper develops a double side-band suppressed carrier (DSB-SC) signal model for use with NLR-based calibration methods. The DSB-SC model not only provides a useful signal for calibration, it also demonstrates the model flexibility inherent to nonlinear regression techniques. Simulations illustrate the effectiveness of the DSB-SC signal model for the calibration of I/Q sensors.

Categories:
5.7: Sig. and Sys. Modeling, 5.5 Parameter Est.

1. INTRODUCTION

In [1], Green/Anderson-Sprecher/Pierre present a nonlinear regression (NLR) -based method to calibrate gain and phase mismatch between the in-phase (I) and quadrature (Q) branches of a quadrature receiver. The method is effective, easy to implement, and provides excellent techniques for on-line error assessment. Unfortunately, [1] only presents a single model: a pure sinusoidal test signal. The pure sinusoidal model can be somewhat restrictive, and it does not display the model flexibility inherent to nonlinear regression techniques. This paper develops another signal model for NLR calibration: the double side-band suppressed carrier (DSB-SC) test signal. Derivation of the DSB-SC model also demonstrates the model flexibility of the NLR calibration technique.

It is worthwhile to note that other effective I/Q mismatch calibration procedures exist. Churchill/Ogar/Thompson provide a standard deterministic technique referred to as local test signal injection [2]. Pierre/Fuhrmann furnish a method based upon quadrature detection to determine relative gain and phase mismatch [3]. Macleod [4] presents a Fourier-based wideband calibration technique that, like [2], uses direct test-signal injection. The method of Lee [5] is also based on direct injection of calibration signals.

The NLR calibration techniques in [1] provide several advantages over existing methods including modest model assumptions, accommodation of non-uniformly sampled or missing calibration data, effective on-line performance assessment, and model flexibility. Furthermore, the NLR-based techniques calibrate receivers in normal operating environments. That is, test signals are transmitted to receivers according to field design – while direct test signal injection is supported, it is not necessary.

2. NONLINEAR REGRESSION BASICS

For processes that follow a NLR model, observations are expressed according to:

$$Y_n = f\left(\boldsymbol{X}_n, \boldsymbol{\beta}\right) + \varepsilon_n, \tag{1}$$

where Y_n is the n^{th} observed value; $f\left(\cdot\right)$ is a nonlinear function of a known predictor vector, $\boldsymbol{X}_n$, and an unknown parameter vector, $\boldsymbol{\beta}$; and ε_n is additive, zero-mean, uncorrelated noise.

The unknown parameter vector, $\boldsymbol{\beta}$, is estimated using techniques such as steepest descent or Gauss-Newton. In the Gauss-Newton method, parameter estimates are iteratively updated according to:

$$\hat{\boldsymbol{\beta}}^{(i+1)} = \hat{\boldsymbol{\beta}}^{(i)} + \left(\boldsymbol{D}^{(i)\dagger}\boldsymbol{D}^{(i)}\right)^{-1}\boldsymbol{D}^{(i)\dagger}\left(\boldsymbol{Y} - \boldsymbol{f}^{(i)}\right), \tag{2}$$

where the parenthetical superscript indicates iteration, † denotes the complex conjugate transpose, $\hat{\boldsymbol{\beta}}^{(i)}$ is a length P vector estimate of the unknown parameters, $\boldsymbol{Y}$ is the length N observation vector, $\boldsymbol{D}^{(i)}$ is the N by

P Jacobian with elements $D_{np}^{(i)} = \left[\frac{\partial f(\boldsymbol{X}_n,\boldsymbol{\beta})}{\partial \beta_p}\right]_{\boldsymbol{\beta}=\hat{\boldsymbol{\beta}}^{(i)}}$, and $\boldsymbol{f}^{(i)}$ is the length N estimated response vector with elements $f_n^{(i)} = f\left(\boldsymbol{X}_n, \hat{\boldsymbol{\beta}}^{(i)}\right)$. Details are in [1].

In the NLR context, there exist several effective methods to ascertain estimator performance. Provided independent, normal errors and a reasonable sample size, α-level confidence intervals are straightforward:

$$\left[\hat{\beta}_p - t_{N-P} s\left\{\hat{\beta}_p\right\}, \hat{\beta}_p + t_{N-P} s\left\{\hat{\beta}_p\right\}\right], \qquad (3)$$

where $t_{N-P}(1-\alpha/2)$ is the $(1-\alpha/2)100$ percentile of the student-t distribution with $N-P$ degrees of freedom.

Resampling techniques, such as the jackknife or the bootstrap, have no underlying assumptions regarding sample size or normality of errors, and they provide effective alternatives to (3). Details for jackknife and bootstrap inferences are given in [1].

3. DSB-SC SIGNAL MODEL

Figure 1 illustrates a standard quadrature receiver. The gain and phase errors are modeled by the impulse response functions h_I and h_Q, for the I and Q branches respectively. This approach allows errors to be frequency dependent as shown by the frequency-domain representations of the response functions: $H_I(\omega) = G_I(\omega)\exp(-j\psi_I(\omega))$ and $H_Q(\omega) = G_Q(\omega)\exp(-j\psi_Q(\omega))$. Although the errors are modeled as frequency dependent, it is reasonable to assume that the gain and phase errors are approximately constant over narrow frequency bands.

The DSB-SC test signal provides a common transmission signal that can be used for NLR-based receiver calibration. For this model, the receiver is assumed to be omni-directional. Essentially, DSB-SC involves a sinusoidal message signal of frequency ω_m modulated by a sinusoidal carrier of frequency ω_c. Provided the local oscillator shown in Figure 1 is set to the carrier frequency, the message signal is reduced to baseband. In a manner similar to [1], the gain and phase terms are grouped together and the receiver output is given as:

$$\begin{aligned} y(t; I_I, I_Q) = \\ & I_I\left(A(\omega_m)\cos(\psi)\cos(\omega_m t + \alpha(\omega_m))\right) + \\ & I_Q\left(B(\omega_m)\sin(\psi)\cos(\omega_m t + \beta(\omega_m))\right) + \varepsilon(t), \end{aligned} \qquad (4)$$

where additive system noise is designated by $\varepsilon(t)$ and each I serves as an indicator function. The indicator functions provide a way to "stack" observations from different branches and different sources. In this case, $I_I = 1$ and $I_Q = 0$ when representing data from the in-phase branch; $I_I = 0$ and $I_Q = 1$ when representing data from the quadrature branch.

In (4), the grouped gain parameters, $A(\omega_m)$ and $B(\omega_m)$, include contributions from the unknown test signal gain as well as the unknown gains of each individual branch. Similarly, the grouped parameters, $\alpha(\omega_m)$ and $\beta(\omega_m)$, represent phase contributions from the test signal as well as the receiver. Relative phase and gain mismatch error are defined according to $A(\omega)/B(\omega)$ and $\alpha(\omega) - \beta(\omega)$, respectively. For the sake of simplicity, local oscillator deviations are not included in this model. Allowance can be made for local oscillator errors, but the errors cannot simply be grouped together; the model is thus more complex.

An unknown parameter ψ is also introduced by this model, and it presents difficulties when using NLR methods. First, since ψ is shared in both branches, indicator functions are required to couple the equations together. Second, observations from (4) alone are insufficient to estimate the unknown parameters. The system is rank deficient and thus possesses an infinite number of possible solutions.

One way to remedy this situation is to collect data from two independent source locations. Observations can then be expressed according to:

$$\begin{aligned} y(t; I_I, I_Q, I_{S1}, I_{S2}) = \\ & I_{S1} I_I\left(A(\omega_m)\cos(\psi_{S1})\cos(\omega_m t + \alpha(\omega_m))\right) + \\ & I_{S1} I_Q\left(B(\omega_m)\sin(\psi_{S1})\cos(\omega_m t + \beta(\omega_m))\right) + \\ & I_{S2} I_I\left(A(\omega_m)\cos(\psi_{S2})\cos(\omega_m t + \alpha(\omega_m) + \gamma)\right) + \\ & I_{S2} I_Q\left(B(\omega_m)\sin(\psi_{S2})\cos(\omega_m t + \beta(\omega_m) + \gamma)\right) + \\ & \varepsilon(t), \end{aligned} \qquad (5)$$

where the subscripts $S1$ and $S2$ identify which source is being used. Separate indicator functions are required to distinguish data from each source location. Additionally, ψ depends on source location and the parameter γ appears to allow for phase mismatch between sources. Although the addition of a second source location complicates the nonlinear model, the system is now full rank and estimates of the parameters can be obtained.

The gain and phase parameters as well as ψ affect the SNR of the system, and the SNR is rarely the same between branches. Because it is a function of unknowns, SNR is itself unknown. Note that certain values of ψ seriously degrade the SNR for a particular branch when using model (5). This reduces estimator efficiency for parameters associated with that branch. As an extreme example, if ψ is equal to zero, no meaningful estimate of the Q branch parameters can be obtained. Estimator performance measures will indicate

when ψ is unacceptable. Recommendations in [1] regarding system sampling should be followed as well to ensure good parameter estimates.

The models given in (4) and (5) are somewhat generalized. Some DSB-SC systems, such as those which utilize a Costas loop to lock onto the carrier frequency, may require model modifications to be entirely accurate. When using the DSB-SC model in (4), phase estimates are modulo 180 degrees. This is a consequence of the π-periodicity of the cosine function. The consequence, of course, is a potential 180 ambiguity in the estimate of the receiver's phase mismatch. For single sensor systems, this ambiguity generally has no detrimental effects on system performance. In sensor array systems, iterative inter-element calibration techniques are required. Details regarding inter-element calibration, along with appropriate references, are in [1].

4. SIMULATIONS AND RESULTS

Table 1 provides the simulation results of NLR calibration that utilizes the double side-band suppressed carrier model of (5) with independent, normally distributed errors ($\sigma_\varepsilon^2 = 0.01$). For this simulation, a relatively small sample size of 80, or 20 observations per branch and source, is used. Note also, with this model some nuisance parameters, such as γ and the ψ's, must be estimated in order to estimate the gain and phase mismatch of the receiver.

The parameter estimates empirically appear to be unbiased or nearly so, and the performance measures based on (3), jackknife methods, and the bootstrap all provide comparable results. As previously discussed, some values of ψ degrade the SNR of one branch more than the other branch. This phenomenon is emphasized in Table 1 by realizing that the standard deviations and confidence intervals of the parameter estimates between branches differ significantly.

Suppose system specifications require gain calibration within one-percent of the true values. As evidenced by Table 1, a sample consisting of 20 observations per branch per source is insufficient. Table 2 illustrates the effect of varying sample size on estimator performance. Clearly, the case of 2000 samples per branch per source, for a total of 8000 observations, results in estimates that are within tolerance requirements. By monitoring estimates using large sample, jackknife, or bootstrap methods, it is easy to verify whether or not estimates meet system requirements.

5. CONCLUSIONS

A DSB-SC test signal was developed for NLR-based calibration of gain and phase mismatch in I/Q receivers. The DSB-SC model not only provides a useful, effective calibration signal, but it also helps illustrate the model flexibility inherent to NLR-based methods. Simulations illustrate DSB-SC model effectiveness for receiver calibration. Simulations also demonstrate the use of large-sample, jackknife, and bootstrap techniques to monitor estimator performance.

6. REFERENCES

[1] Green, R. A., Anderson-Sprecher, R. A., and Pierre, J. W. "Quadrature Receiver Mismatch Calibration," submitted for second review, *IEEE Transactions on Signal Processing,* July, 1998.

[2] F. Churchill, G. Ogar, and B. Thompson, "The Correction of I and Q Errors in a Coherent Processor," *IEEE Trans. AES*, vol. AES-17, no. 1, pp. 131-137, January 1981.

[3] J. Pierre and D. Fuhrmann, "Considerations in Autocalibration of Quadrature Receivers," *Proc. ICASSP '95*, pp. 1900-1903, Detroit, Michigan, May 1995.

[4] M. D. Macleod, "Fast Calibration of IQ Digitizer Systems," *Electrical Eng.,* pp. 41-45, 1990.

[5] J. P. Y. Lee, "Wideband I/Q Demodulators: Measurement Technique and Matching Characteristics," *IEE Proc. Radar, Sonar Navig.,* Vol. 143, No. 5, October 1996.

[6] J. Neter, M. H. Kutner, C. J. Nachtsheim, and W. Wasserman, Applied Linear Statistical Models, 4^{th} Edition, Richard D. Irwin, Inc., pp. 531-559, 1996.

[7] D. M. Bates and D. G. Watts, Nonlinear Regression Analysis and Its Applications, New York's John Wiley & Sons, 1988.

[8] B. Efron, The Jackknife, the Bootstrap, and Other Resampling Plans, CBMS-NSF Regional Conference Series in Applied Mathematics, No. 38, Society for Industrial and Applied Mathematics, 1982.

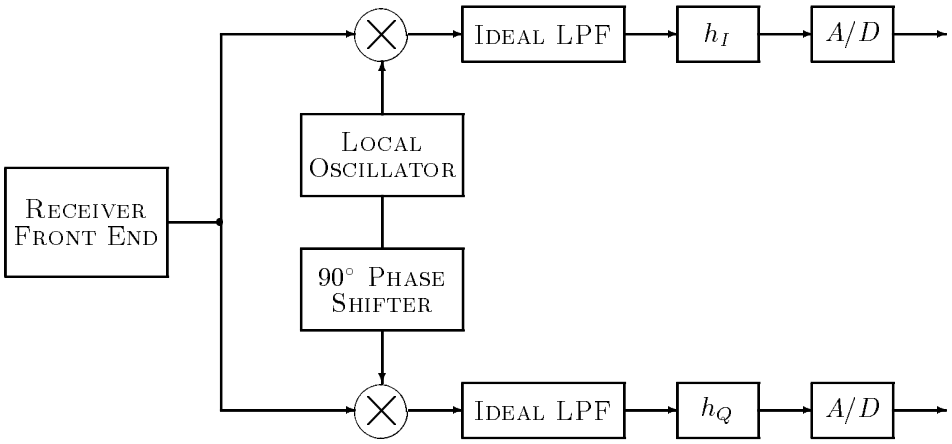

Figure 1: I/Q Receiver with Gain and Phase Imbalances

	True	Est.	EQ. (3)		Jackknife			Bootstrap		
			S.D.	C.I.	BIAS	S.D.	C.I.	BIAS	S.D.	C.I.
A	1.0599	1.1234	0.0977	0.9287 1.3181	0.0102	0.0872	0.9599 1.3073	0.0096	0.0883	0.9571 1.3089
B	1.1041	1.0970	0.0403	1.0167 1.1774	0.0025	0.0372	1.0254 1.1736	0.0026	0.0368	1.0263 1.1729
α	0.1622	0.1061	0.0577	-0.0089 0.2211	0.0006	0.0650	-0.0228 0.2362	0.0012	0.0615	-0.0152 0.2298
β	2.6450	2.6503	0.0308	2.5895 2.7122	0.0002	0.0427	2.5655 2.7355	0.0010	0.0412	2.5692 2.7334

Table 1: DSB-SC Test Signal, $N = 80$, and Measures of Performance

	True	$N = 80$		$N = 800$		$N = 8000$	
		Est.	C.I.	Est.	C.I.	Est.	C.I.
A	1.0599	1.1234	0.9287 1.3181	1.0919	1.0269 1.1569	1.0511	1.0341 1.0682
B	1.1041	1.0970	1.0167 1.1774	1.0750	1.0489 1.1011	1.1105	1.1026 1.1184
α	0.1622	0.1061	-0.0089 0.2211	0.1751	0.1396 0.2106	0.1698	0.1591 0.1805
β	2.6450	2.6503	2.5895 2.7122	2.6410	2.6218 2.6602	2.6476	2.6420 2.6533

Table 2: DSB-SC Performance, Equation (3), and Varying Sample Size